FABRICATION AND OPTICAL CHARACTERISTICS OF OPAL PHOTONIC CRYSTAL FILMS AND HETEROSTRUCTURES

V.S. Mukharovska*, M.P. Derhachov, V.M. Moiseyenko

Oles Honchar Dnipro National University, Dnipro, Ukraine
**e-mail: mukharovska@ffeks.dnu.edu.ua*

The relevance of fabrication and investigation of opals and opal-based structures is due to their ability to control the emission and propagation of light. Using the method of vertically moving meniscus we obtain both single opal films and two-film heterostructures. By examining reflectance spectra, we analyze the influence of the ratio of synthesis components on silica particle diameter. Features of the heterostructure reflectance spectrum are also discussed by considering the contribution of light scattering by the interface.

Keywords: photonic crystals, monodisperse silica particles, synthesis, opal heterostructure, reflectance, Bragg diffraction.

Received 09.11.2022; Received in revised form 10.12.2022; Accepted 23.12.2022

1. Introduction

Current trends in optoelectronics require materials that ensure confident control over the spectral and spatial distribution of optical radiation energy. One of these materials is photonic crystals (PhCs), artificial structures with a period of permittivity modulation close to light wavelengths. PhCs have the unique ability to create photonic band gaps (PhBG) where electromagnetic waves cannot propagate due to destructive interference. As a result, PhCs are increasingly used as the basis for creating nanophotonic devices, sensors, and lasers. [1-3].

One of the prototypes of 3D PhCs is a synthetic opal composed of sequential layers of close-packed monodisperse spherical silica particles. Opal films are of great interest here due to wider technological abilities of varying their properties, lower defect concentration and shorter fabrication time [4, 5]. Their planar structure allows to extend the fields of the PhCs application to deformation imaging [6], silicon photovoltaics [7], and anti-counterfeiting technology [8] in addition to the above.

Furthermore, opal films are promising material for creation of controlled defects. As a defect leads to an eigenstate in the PhBG, it would be possible to provide directed emission in the narrow spectral range by forming a straight line of such defects inside an opal. However, creation of predetermined defects becomes challenging for bulk opals. Nevertheless, if a heterostructure is created out of two opal films, then the interface is itself a planar defect. This approach makes it possible to obtain laser generation from a single PhC chip, as well as to fabricate multifrequency optical Bragg filters, PhC sensors or superlattices [9, 10].

In this paper, we examinate the effect of the synthesis component concentration on the diameter of monodisperse spherical silica particles and work out the technology for obtaining opal heterostructures with their further parametrisation by optical spectroscopy technique.

2. Sample fabrication and experimental technique

The fabrication of opal film samples involved the synthesis of silicate particles (SPs) and their subsequent deposition onto substrates. SPs were produced by the hydrolysis of tetraethyl orthosilicate $Si(OC_2H_5)_4$ (TEOS) in an ethanol–water solution in the presence of ammonia hydroxide as catalyst. Thereupon particles were deposited on a glass substrate by the vertically moving meniscus method (Fig. 1a). SPs formed a face-centred cubic (fcc) lattice with the lattice direction [111] perpendicular to the film surface [11]. The film growth process was carried out under the isothermal conditions at 25 °C with the subsequent annealing at 100 ^{0}C for 6 hours to increase mechanical stability.

To fabricate heterostructures, SPs with another diameter were prepared by the multistage

Stöber method with using already synthesized particles as seeds [12]. In this respect, portion of the suspension was diluted in water–ethanol–ammonium mixed solvent of the same compound and additional quantity of TEOS. Depositing new SPs, we obtained the second film crystallized on the first one acting like a substrate. Upon the crystallization all the samples were annealed at 450 °C for 3 hours to remove physically adsorbed water and organic residues [13].

Reflection spectra of samples were measured at different angles θ with respect to normal to the growth surface (Fig. 1b). All the spectra were obtained by using a modified spectrometer based on a double monochromator DFS-12 within the 400 – 650 nm range. Reflectance coefficients were derived from the corresponding spectra by dividing them by the emission spectrum of incandescent lamp used for sample illumination. The light beam diameter on the sample surface was no more than 1 mm. An error in angle setting did not exceed 1.5°, and an accuracy in defining spectral position was ±0.15 nm.

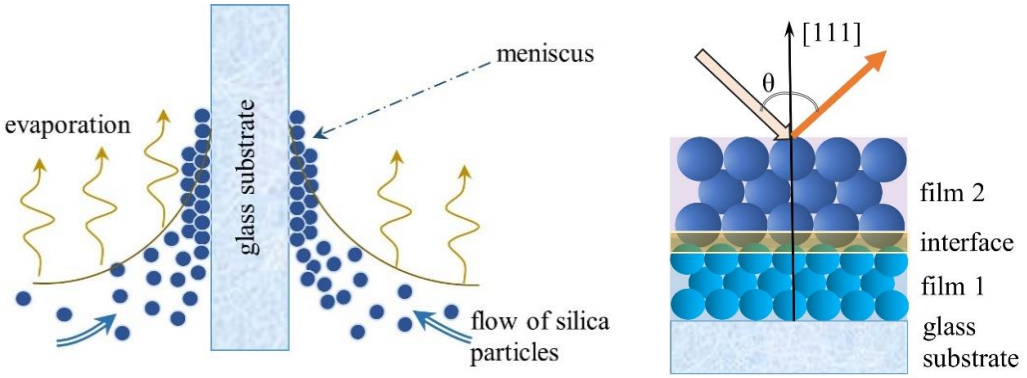

Fig. 1. Fabrication and measurement schemes: (a) – growing the opal film by the method of vertically moving meniscus; (b) – obtaining the reflection spectrum of the two-film opal heterostructure.

3. Results and discussion

Typical angular dependence of the opal film reflection spectrum is shown by the curves 1, 2, and 3 in Fig. 2. Since opal is a structure with dielectric modulation on the nanometer scale, its reflection spectrum is due to the Bragg diffraction of light on sets of the planes (*hkl*) of fcc lattice. This process can be described by the Laue equation, $\mathbf{k} + \mathbf{G}_{hkl} = \mathbf{k}'$, where $\mathbf{k}$ and $\mathbf{k}'$ are wavevectors of incident and reflected beams respectively, and $\mathbf{G}_{hkl}$ is the corresponding reciprocal lattice vector. For light diffraction on the planes (111), usually of the first order one, the reflectance maximum position λ_m is derived from the Laue equation as follows

$$\lambda_m = 2d_{111}\sqrt{n_{eff}^2 - \sin^2\theta} \qquad (1)$$

where d_{111} is the interplanar (111) spacing and n_{eff} is the effective refraction index. The latter is defined as square root of the sum of partial permittivities of silica and air and assigned as 1.27 in our calculations. In the coordinate system $\{n_{eff}^2 - \sin^2\theta;\ \lambda_m^2\}$, the angular dependence of the reflectance maximum is well described by the linear approximation with zero intercept (the inset in Fig. 1), and d_{111} is derived from the slope value. According to $D = d_{111}\ (3/2)^{1/2}$, mean SP diameter D for different mixture compositions can be calculated (Table 1). The value of the relative reflectance bandwidth, not exceeding 10%, indicates a low dispersion of particle diameters within several nanometers.

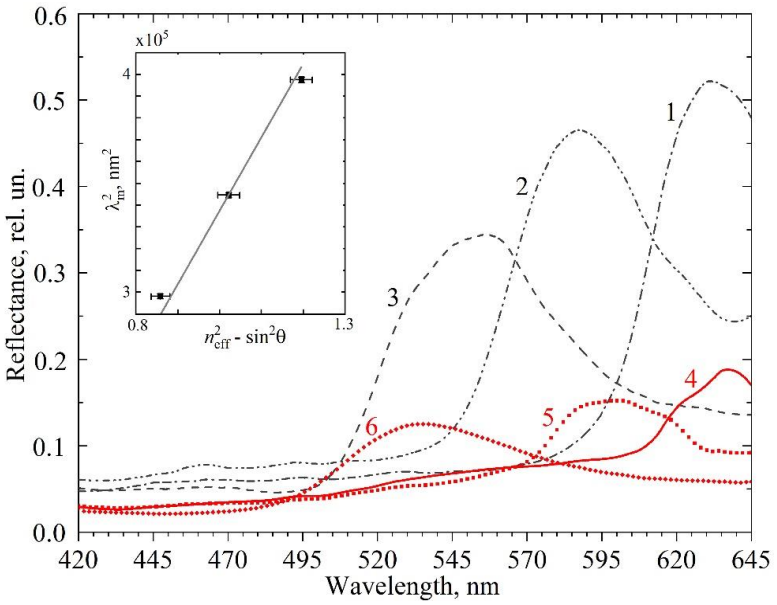

Fig. 2. The single film (1-3) and heterostructure (4-6) spectra at θ=40° (1, 4), 50° (2, 5), 60° (3) and 65° (6). The single and bottom heterostructure films correspond to the mixture composition labelled as N7 in Table 1, the top film is related to the composition W3T. Linear approximation of angular dependence of the reflectance maximum position for the N7 single film is presented in the inset.

Table 1

The mixture composition used for the synthesis silica particles and mean silica particle diameter

Series label	Volume, 10^{-6} m^3				*D*, nm
	H_2O	C_2H_5OH (96 %)	$Si(OC_2H_5)_4$ (98 %)	NH_4OH (25 %)	
N7	12	100	4.8	42	356
W	7	100	7	13	246
W10	7	100	7	13 (10 %)	250
W2T	7	100	9.5	13	270
W3T	7	100	7 (+ 3.5)*	13	– **
AM4	7	100	7	13 (+4)*	– **

* added after the first stage of synthesis (by using the multistage Stöber method)
** not determined for a single film, used as top film in the heterostructure with bottom N7 film

As can be seen from Table 1, the combined reduction in water and ammonia together with increasing TEOS leads to an essential decrease in the SP diameter. At the same time, increasing the amount of TEOS, while keeping all other parameters unchanged, contributes to an increase in the SP diameter. As afore stated, the facilitated synthesis of silica particles with diameters like N7 composition is used for growing bottom films in heterostructures.

Angular dependence of the N7 + W3T heterostructure reflectance is represented by the curves 4, 5, and 6 in Fig. 2. As in the spectra of single films, the reflection band is shifted towards the shorter wavelengths with increasing angle of light incidence. It can be explained by assuming the heterostructure reflection spectrum as the sum of the reflection spectra of top and bottom films. In this case, the "red side" shift of the heterostructure band compared to that of N7 single film at the same angle θ indicates the larger SP diameter in W3T top film (Fig. 2). The band broadening with increasing θ could be caused by different angular dependence of reflection bands for top and bottom films, in accordance with Eq. 1. It should also be noted that the heterostructure reflectance is much lower than that of a single opal film. It is most likely due to additional light scattering at the interface in the heterostructure.

4. Conclusions

Angular dependence of the single opal film reflectance is well described within the framework of the Bragg light diffraction and can be used to control the SP diameter. The latter is essentially changed by varying the TEOS and ammonia hydroxide concentrations, especially with using the multistage Stöber method. Opal heterostructure obtained by this method exhibits angular dependence of reflectance generally like that of single film, namely, a "blue shift" of reflectance maximum with increasing the angle of light incidence. However, its spectrum can rather be seen as a superposition of the spectra of the films composing the structure, considering the significant contribution of the interface to light scattering and attenuation of the reflected light beam. The obtained heterostructures can be used as templates for creating laser-active systems by infiltrating them with an appropriate substance.

References

1. **Sharma, A.** A review on photonic crystal based all-optical logic decoder: linear and nonlinear perspectives / A. Sharma, K. Goswami, H. Mondal, T. Datta, M. Sen // Optical and Quantum Electronics. – 2022. – Vol. 54, No. 2. – P. 90 (24).

2. **Li, T.** Recent advances in photonic crystal-based sensors / T.Li, G. Liu, H. Kong, G. Yang, G. Wei, X. Zhou // Coord. Chem. Rev. – 2023. – Vol. 475. – P. 214909 – 31.

3. **Fu, Y.** Distributed feedback organic lasing in photonic crystals / Y. Fu, T. Zhai // Frontiers of Optoelectronics. – 2020. – Vol. 13. – P. 18 – 34.

4. **Panfilova, E.V.** Automation of the opal colloidal films obtaining processes / E.V. Panfilova, V.A. Dyubanov // In Lecture Notes in Electrical Engineering. Ed. by A. Radionov, A. Karandaev. – Springer (Cham), 2020. – P. 1044 – 1052.

5. **Muldarisnur, M.** Structure and optical properties of opal films made by an out-of-plane electric field-assisted capillary deposition method / M. Muldarisnur, F. Marlow // ACS Omega. – 2022. – Vol. 7. – P. 8084 – 8090.

6. **Yang, Z.** Availability of opal photonic crystal films for visualizing heterogeneous strain evolution in steels: Example of Lüders deformation / Z. Yang, M. Koyama, H. Fudouzi, T. Hojo, E. Akiyama // ISIJ International. – 2020. – Vol. 60. – P. 2604 – 2608.

7. **O'Brien, P.G.** Silicon photovoltaics using conducting photonic crystal back-reflectors / P.G. O'Brien, N.P. Kherani, A. Chutinan, G.A. Ozin, S. John, S. Zukotynski // Advanced Materials. – 2008. – Vol. 20. – P. 1577 – 1582.

8. **Winter, T.** Dye-loaded mechanochromic and pH-responsive elastomeric opal films / T. Winter, A. Boehm, V. Presser, M. Gallei // Macromol Rapid Commun. – 2021. – Vol. 42. – 2000557 – 7.

9. **Plekhanov, A.I.** Functional properties of photonic crystals on the basis of single-crystal opal films // In Photonic Crystals: Optical Properties, Fabrication and Applications. Ed. by W.L. Dahl. – Nova Science Publishers: New York. – 2011. – P. 215 –224.

10. **Kuchyanov, A.S.** Laser generation in opal-like single-crystal and heterostructure photonic crystals / A.S. Kuchyanov, A.I. Plekhanov // Optoelectronics, Instrumentation and Data Processing. – 2016. – Vol. 52, No. 6. – P. 96 – 102.

11. **Sinitskii, A.S.** Silica photonic crystals: synthesis and optical properties / A.S. Sinitskii, A.V. Knot'ko, Yu.D. Tretyakov // Solid State Ion. – 2004. – Vol. 172. – P. 477 – 479.

12. **Masalov, V.M.** Colloidal particles of silicon dioxide for the formation of opal-like structures / V.M. Masalov, N.S. Sukhinina, G.A. Emel'chenko // Physics of the Solid State. – 2011. – Vol. 53. – P. 1135 – 1139.

13. **Samarov, E.N.** Structural modification of synthetic opals during thermal treatment / E.N. Samarov, A.D. Mokrushin, V.M. Masalov, G.E. Abrosimova, G.A. Emel'chenko // Physics of the Solid State. – 2006. – Vol. 48. – P. 1280 – 1283.